In-beam γ-ray spectroscopy of ^{63}Mn

T. Baugher,[1,2,3] A. Gade,[1,2] R. V. F. Janssens,[4] S. M. Lenzi,[5] D. Bazin,[1] M. P. Carpenter,[4] C. J. Chiara,[4,6] A. N. Deacon,[7] S. J. Freeman,[7] G. F. Grinyer,[8] C. R. Hoffman,[4] B. P. Kay,[4] F. G. Kondev,[9] T. Lauritsen,[4] E. M. Lunderberg,[1,2] S. McDaniel,[1,2] K. C. Meierbachtol,[1,10] A. Ratkiewicz,[1,2] S. R. Stroberg,[1,2] K. A. Walsh,[1,2] D. Weisshaar,[1] and S. Zhu[4]

[1]*National Superconducting Cyclotron Laboratory, Michigan State University, East Lansing, Michigan 48824, USA*
[2]*Department of Physics and Astronomy, Michigan State University, East Lansing, Michigan 48824, USA*
[3]*Department of Physics and Astronomy, Rutgers University, Piscataway, New Jersey 08854, USA*
[4]*Physics Division, Argonne National Laboratory, Argonne, Illinois 60439, USA*
[5]*Dipartimento di Fisica e Astronomia dell'Università and INFN, Sezione di Padova, I-35131 Padova, Italy*
[6]*Department of Chemistry and Biochemistry, University of Maryland, College Park, Maryland 20742, USA*
[7]*School of Physics and Astronomy, University of Manchester, Manchester M13 9PL, United Kingdom*
[8]*Grand Accélérateur National d'Ions Lourds (GANIL), CEA/DSM-CNRS/IN2P3, Bvd Henri Becquerel, 14076 Caen, France*
[9]*Nuclear Engineering Division, Argonne National Laboratory, Argonne, Illinois 60439, USA*
[10]*Department of Chemistry, Michigan State University, East Lansing, Michigan 48824, USA*

(Received 24 March 2014; revised manuscript received 1 December 2015; published 21 January 2016)

Background: Neutron-rich, even-mass chromium and iron isotopes approaching neutron number $N = 40$ have been important benchmarks in the development of shell-model effective interactions incorporating the effects of shell evolution in the exotic regime. Odd-mass manganese nuclei have received less attention, but provide important and complementary sensitivity to these interactions.

Purpose: We report the observation of two new γ-ray transitions in ^{63}Mn, which establish the $(9/2^-)$ and $(11/2^-)$ levels on top of the previously known $(7/2^-)$ first-excited state. The lifetime for the $(7/2^-)$ and $(9/2^-)$ excited states were determined for the first time, while an upper limit could be established for the $(11/2^-)$ level.

Method: Excited states in ^{63}Mn have been populated in inelastic scattering from a ^{9}Be target and in the fragmentation of ^{65}Fe. $\gamma\gamma$ coincidence relationships were used to establish the decay level scheme. A Doppler line-shape analysis for the Doppler-broadened $(7/2^-) \rightarrow 5/2^-$, $(9/2^-) \rightarrow (7/2^-)$, and $(11/2^-) \rightarrow (9/2^-)$ transitions was used to determine (limits for) the corresponding excited-state lifetimes.

Results: The low-lying level scheme and the excited-state lifetimes were compared with large-scale shell-model calculations using different model spaces and effective interactions in order to isolate important aspects of shell evolution in this region of structural change.

Conclusions: While the theoretical $(7/2^-)$ and $(9/2^-)$ excitation energies show little dependence on the model space, the calculated lifetime of the $(7/2^-)$ level and calculated energy of the $(11/2^-)$ level reveal the importance of including the neutron $g_{9/2}$ and $d_{5/2}$ orbitals in the model space. The LNPS effective shell-model interaction provides the best overall agreement with the new data.

DOI: 10.1103/PhysRevC.93.014313

I. INTRODUCTION

Nuclear shell structure—well-established for nuclei near the valley of β stability—has been observed to change in the exotic regime of neutron-rich nuclei [1,2]. Driving forces behind shell evolution and structural change at large isospin are the central and tensor interactions [3,4]. In the region below ^{68}Ni, the energy spacing between the neutron fp shell and the $g_{9/2}$ orbital at $N = 40$ has been of particular interest. An $N = 40$ subshell gap may be suspected, based on the large 2^+ energy and small $B(E2)$ value of ^{68}Ni [5]; however, in the iron and chromium isotopic chains, with just two or four protons less than nickel, collectivity rapidly develops [6–11]. This region of structural change is a challenging testing ground for nuclear models that aim to incorporate the drivers of structural evolution away from stability.

Much has been learned about the region below ^{68}Ni from studies of collectivity in even-even chromium, iron, and nickel isotopes. In contrast to the high 2_1^+ energy in ^{68}Ni, the energies of the 2_1^+ states of the neutron-rich iron isotopes decline at least out to $N = 42$, ^{68}Fe [7,12], and the energy of the 2_1^+ level in ^{64}Cr is the lowest known in the region [8]. $B(E2)$ values determined via intermediate-energy Coulomb excitation [10,11] and excited-state lifetime measurements [9] quantified further the collectivity in the even-mass chromium and iron isotopes. Only state-of-the-art shell-model calculations which included the $\nu 0g_{9/2}$ and $\nu 1d_{5/2}$ orbitals in the model space reproduced the accumulating experimental observations regarding collectivity [9–11,13]. Studies of odd-mass nuclei provide complementary information and sensitively test aspects relevant for the effective interactions developed for this region of rapid structural change [14].

Between iron and chromium lie the $(Z = 25)$ manganese isotopes. The neutron-rich, odd-even isotopes ^{59,61,63}Mn were previously studied via multinucleon transfer by Valiente-Dobón *et al.* [15]. Steppenbeck *et al.* determined the spin-parities of high-spin levels in $^{57-60}$Mn by measuring γ-ray angular distributions following heavy-ion fusion-evaporation reactions [16]. Deep-inelastic processes studied by Chiara *et al.* revealed new levels in ^{61,62}Mn [17], and excited states in ^{61}Mn were also populated via β decay by Crawford *et al.* [18]. Aside from the $(7/2_1^-) \rightarrow 5/2_1^-$ transition from

the first excited state to the ground state, relatively little is known about the structure of ^{63}Mn. Several transitions were reported in the β decay from ^{63}Cr to ^{63}Mn by Gaudefroy *et al.* [19], but weak statistics prevented the construction of a level scheme and the transitions remain unplaced. Shell-model calculations using the GXPF1A [20,21] and fpg [5] effective interactions (GXPF1A is restricted to the fp shell for protons and neutrons, fpg includes the neutron $g_{9/2}$ orbital) reproduce the energy of the first excited $(7/2^-)$ state in ^{63}Mn to a reasonable degree, as shown in Refs. [15,18]. A recent laser spectroscopy measurement deduced from the hyperfine structure $J = 5/2$ for the ^{63}Mn ground state [22]. Beyond this, however, there are larger differences in the predicted level densities below 1 MeV for the different model spaces; this is particularly apparent in the comparison provided in the work of Ref. [18]. Complementary experimental information on transition probabilities in ^{63}Mn has not been available to this point.

We report on the observation of new transitions in ^{63}Mn and on the determination of excited-state lifetimes from a Doppler line-shape analysis using in-beam γ-ray spectroscopy. Combined with state-of-the-art shell-model calculations [13], we discuss the influence of the $0g_{9/2}$ and $1d_{5/2}$ neutron orbitals on structure in this region.

II. EXPERIMENT AND RESULTS

The measurement was performed at the National Superconducting Cyclotron Laboratory (NSCL). From a primary beam of ^{76}Ge, a secondary one containing ^{63}Mn was produced via projectile fragmentation at 130 MeV/nucleon on a 493-mg/cm^2 ^{9}Be production target located at the entrance of the A1900 fragment separator [23]. The resulting secondary-beam cocktail was purified using a 240-mg/cm^2 Al wedge at the center of the separator with a momentum acceptance of 2.6%. The A1900 separator was set to optimize the yield of ^{62}Cr, but ^{63}Mn was transmitted at comparable intensity.

The secondary beam containing ^{63}Mn was guided onto a 370-mg/cm^2 ^{9}Be reaction target located at the pivot point of the S800 magnetic spectrograph [24] to induce reactions at a beam energy of 84 MeV/nucleon. The spectrograph was set to accept inelastically scattered projectiles, but contributions to the production of ^{63}Mn from fragmentation of ^{65}Fe, which was the most abundant species in the cocktail beam, could not be excluded.

The focal plane of the spectrograph was equipped with the standard set of detectors used for event-by-event identification of the particles emerging from the target [25]. The ionization chamber measured the energy loss of the reaction residues and, combined with the event-by-event time-of-flight through the system, the particle identification matrix shown in Fig. 1 was constructed to select the species of interest.

The target was surrounded by the segmented germanium array (SeGA) consisting of 17, 32-fold segmented high-purity germanium detectors for in-beam γ-ray detection [26]. Seven detectors were mounted in a ring at 37° relative to the beam axis, while the remaining ten equipped a ring at 90°. The high degree of segmentation of the SeGA array allowed an event-by-event Doppler reconstruction of the γ rays emitted in flight

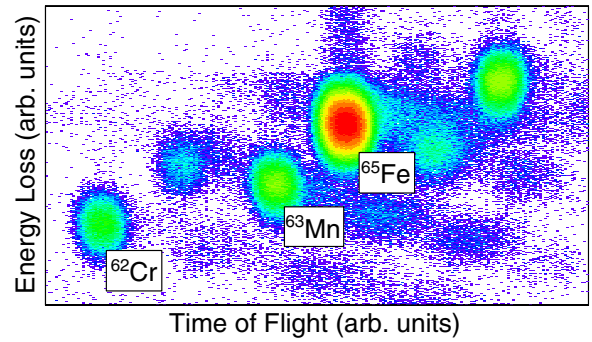

FIG. 1. Particle-identification spectrum for the reaction residues produced at the S800 target position by the incoming projectile beam. The magnetic rigidity of the S800 spectrograph was optimized for the transmission of ^{62}Cr. ^{63}Mn nuclei can be cleanly separated.

by ^{63}Mn nuclei traveling at velocities of $\approx 0.4c$. For each event, the angle used for Doppler reconstruction was deduced from the location of the detector segment with the highest energy deposit. Energy and efficiency calibrations were performed using standard calibration sources. The detection efficiency of SeGA for γ rays emitted in flight, accounting for the Lorentz boost, was evaluated separately for each of the two rings.

The event-by-event, Doppler-corrected γ-ray spectrum of ^{63}Mn is given in Fig. 2. Prominent in the spectrum are γ-ray transitions at 249, 375, and 637 keV. The 249-keV decay was previously attributed to the $(7/2^-_1) \rightarrow 5/2^-_{\text{g.s.}}$ transition [15]. The spin and parity assignments for the and $(7/2^-_1)$ states are based on the systematics of the lighter Mn isotopes [18,27,28], reinforced by shell-model calculations (see below). The 637- and 375-keV transitions had not been reported previously.

γ-rays detected within 600 ns of one another were taken as coincident and stored in a two-dimensional coincidence matrix. Software gates were placed around peaks in the matrix to determine the coincidence relationships between the transitions of interest. Background gates were placed in a peak-free region of the spectrum on the high-energy side of each peak.

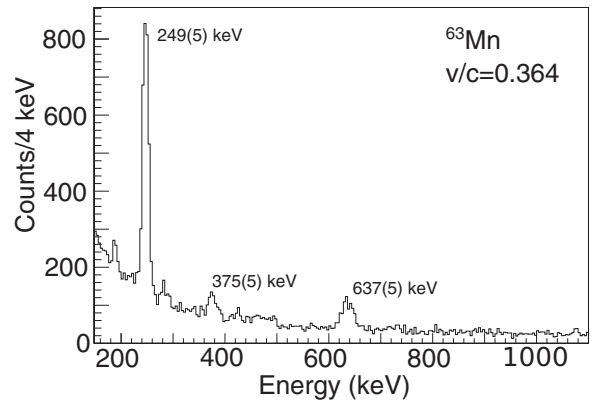

FIG. 2. Event-by-event, Doppler-reconstructed γ-ray spectrum detected by the SeGA array in coincidence with ^{63}Mn reaction products.

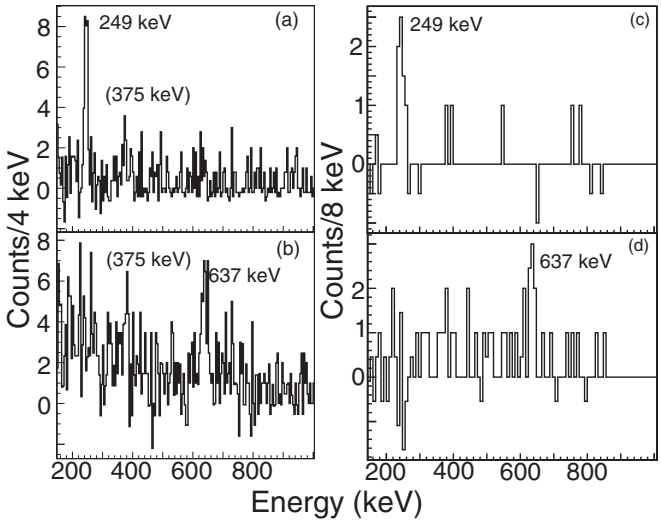

FIG. 3. $\gamma\gamma$ coincidence spectra for ^{63}Mn detected in the SeGA [(a) and (b)] and GRETINA [(c) and (d)] arrays. The top panels [(a) and (c)] are gated on the 637-keV transition, and the bottom panels [(b) and (d)] on the 249-keV γ ray. The two transitions are clearly in coincidence.

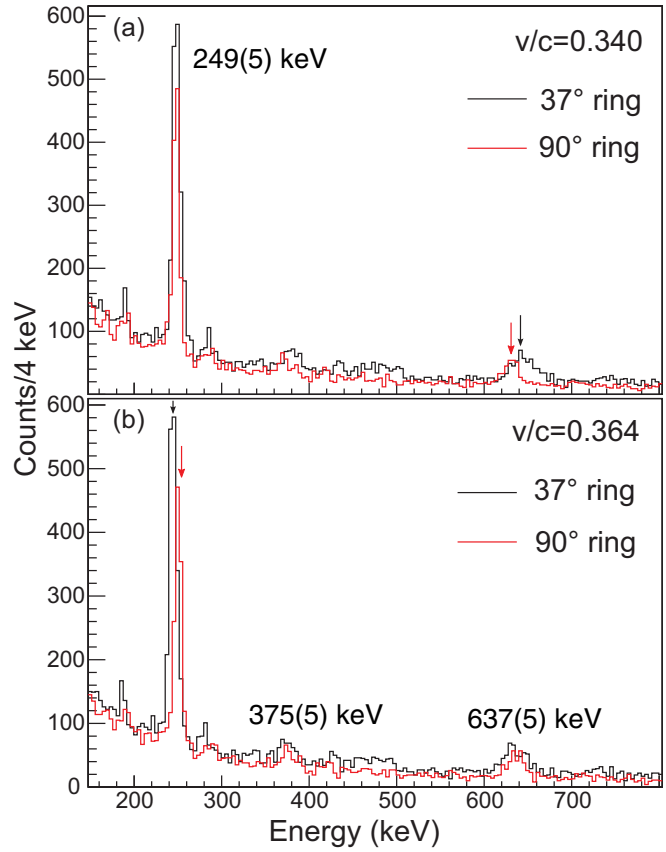

FIG. 4. ^{63}Mn γ-ray spectra for the two rings of the SeGA array. In the top panel, $v/c = 0.340$ was used for the event-by-event Doppler reconstruction of the γ rays emitted in flight, while in the bottom panel $v/c = 0.364$. The position of the peaks in each ring relative to the other is different in each case, illustrating the impact of the excited-state lifetime.

The spectra resulting from the $\gamma\gamma$ coincidence gating are provided in Figs. 3(a) and 3(b). In the spectrum resulting from the gate on the 249-keV transition, the 637-keV γ ray is evident and vice versa. Since the 249-keV transition is known to proceed to the ground state, the 637-keV one is placed directly above the 249-keV level. The resulting 886-keV state is given a tentative spin-parity assignment of $(9/2^-)$, based on the analogy with the level schemes of the lighter Mn isotopes [15], discussed below. Further confirmation of this coincidence relationship was obtained in the calibration setting of an in-beam γ-ray spectroscopy measurement using the same experimental scheme with the GRETINA array [29] instead of SeGA. There, ^{63}Mn was produced in the one-neutron knockout from ^{64}Mn and a small fraction of the momentum distribution entered the S800 focal plane [30]. The same two transitions were observed and confirmed to be in coincidence, as displayed in Figs. 3(c) and 3(d). There is weaker evidence for the 375-keV γ ray being in coincidence with both the 249- and 637-keV transitions in Figs. 3(a) and 3(b). Comparison with the lighter, odd-even Mn isotopes would tentatively suggest an $(11/2^-)$ assignment for the corresponding state.

Figure 4 provides the γ-ray spectra for the individual rings of the SeGA array. In Fig. 4(a), $v/c = 0.340$ was used for the Doppler reconstruction. With this value, the peaks corresponding to the $(7/2^-) \rightarrow 5/2^-$ transition are aligned at 249 keV in both the 37° and 90° rings, while the peaks corresponding to the $(9/2^-) \rightarrow (7/2^-)$ decay are misaligned. On the other hand, with $v/c = 0.364$ in the Doppler reconstruction, the peaks in both rings at 637 keV, corresponding to the $(9/2^-) \rightarrow (7/2^-)$ transition, are aligned, while the peaks for the $(7/2^-) \rightarrow 5/2^-$ transition are now misaligned [see Fig. 4(b)]. This first analysis suggests that the lifetimes of the $(9/2^-)$ and $(11/2^-)$ states are shorter than that of the $(7/2^-)$ level. Since the projectiles continuously lose energy as they traverse the target, on average, a short-lived state is more likely to decay when the projectiles are traveling at higher velocity relative to a longer-lived level that will deexcite after the projectiles have traversed more material, or left the target. Hence, a larger value of v/c is needed in the Doppler reconstruction of a fast transition in order to align the peaks in both rings, while a smaller one is required for a longer-lived level. To quantify the lifetimes of the excited states further, a GEANT4 [31] simulation was used to model the peak shapes and positions of the 375-, 637-, and 249-keV transitions. The excited-state lifetimes τ and energies E of all three states were varied independently and fit to the data in a χ^2-minimization procedure. A linear background was used in the area immediately surrounding the peaks. In this common minimization, the effect of feeding from the states at the top of the cascade was taken into account for the lower-lying states through the simulation and minimization. The χ^2 for each transition was calculated for the fit region surrounding the peak (the area shown in Fig. 5). The lifetimes were subsequently derived from the minimum in χ^2 versus τ plots, and the lifetime corresponding to $\chi^2 + 1$ was taken as the 1σ uncertainty. For the 375-keV transition, only an upper limit could be determined. The upper and lower limits of the observed feeding

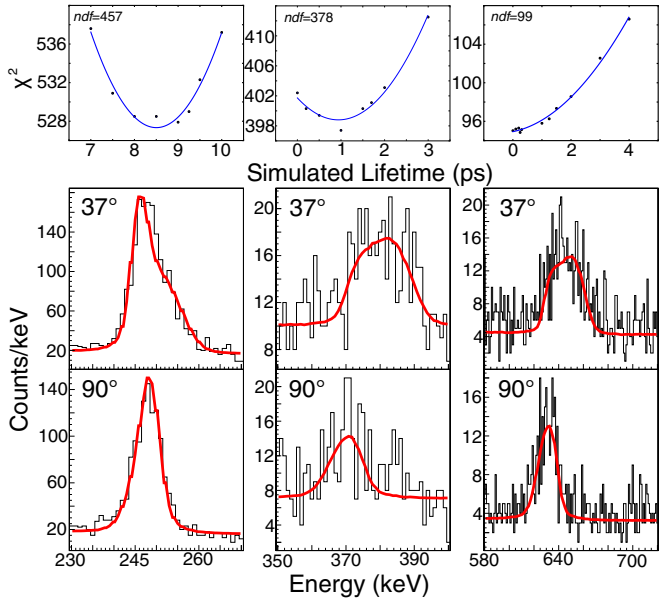

FIG. 5. Fits of simulated (GEANT4) γ-ray transitions (smooth, red curve) to measured spectra (black histogram) used to determine the excited-state lifetimes of levels depopulated by the 249- (left column), 375- (middle column), 637-keV (right column) transitions. The simulated response is the sum of the simulated transitions and a linear background. Top row: reduced-χ^2 values versus simulated lifetime used to determine the best-fit τ value. The number of degrees of the freedom (ndf) entering each lifetime determination is quoted in the χ^2 plots in the top row.

transitions were used to estimate the uncertainties in the fed transitions. Unobserved delayed feeding can only be of weak intensity and would lead to a longer apparent lifetime for the $(9/2^-)$ state than the actual value, herewith amplifying the disagreement with LNPS-fpg and LNPS-fp (see below). The best-fit simulations and corresponding χ^2 versus lifetime plots are presented in Fig. 5. The results are summarized in Table I.

The observation of a firm coincidence between the 637- and 249-keV transitions leads to the level scheme proposed in Fig. 6 with the 375-keV γ ray tentatively placed feeding the $(9/2^-)$ state. For comparison, the level schemes proposed for ^{59,61}Mn by Valiente-Dobón *et al.* [15] are reproduced in Fig. 6 as well. Spin-parity assignments for ^{61,63}Mn in Fig. 6 are tentative and based on systematics of the lighter Mn isotopes, as well as shell-model calculations. The similarities in structure between the isotopes are obvious. In each case, there is a $5/2^-$ ground state and a $7/2^-$ level at low excitation energy, then a larger gap to a $9/2^-$ state with an $11/2^-$ level

TABLE I. Results from the simulations of excited-state lifetimes for the 249-, 637-, and 375-keV transitions in ^{63}Mn.

$J_i^\pi \rightarrow J_f^\pi$	E_γ (keV)	τ (ps)
$(7/2^-) \rightarrow 5/2^-$	249(5)	8.5(0.5)
$(9/2^-) \rightarrow (7/2^-)$	637(5)	0.9(0.6)
$(11/2^-) \rightarrow (9/2^-)$	375(5)	<1

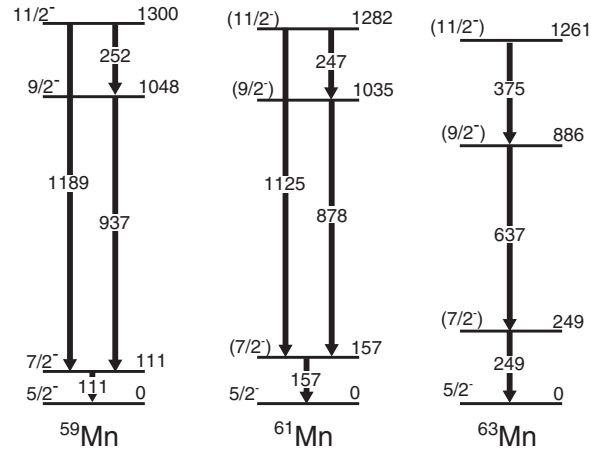

FIG. 6. Comparison of proposed level schemes for ^{59,61,63}Mn for levels below 1.5 MeV. The level schemes for ^{59,61}Mn are taken from [15]. The levels are labeled with spin, parity, and excitation energy in keV. Spin-parity assignments for ^{61,63}Mn are tentative, based on systematics and guided by shell-model calculations. Ground-state spin assignments of $J = 5/2$ were recently confirmed by laser spectroscopy of the hyperfine structure at ISOLDE [22].

above it. In ^{59}Mn, a $15/2^-$ state is observed at nearly 3 MeV in Ref. [16], but is not shown in Fig. 6.

III. DISCUSSION

The proposed level scheme for ^{63}Mn is compared to shell-model calculations in Fig. 7. Negative-parity, yrast levels up to the $11/2^-$ state, and allowed $E2$ and $M1$ transitions were considered. Several calculations were performed using the Lenzi-Nowacki-Poves-Sieja (LNPS) effective interaction [13] with different model spaces. Calculations in the $fpgd$ model space include the fp shell for protons and the $1p_{3/2}$, $1p_{1/2}$, $0f_{5/2}$, $0g_{9/2}$, and $1d_{5/2}$ orbitals for neutrons; they are labeled "LNPS". The fpg model space is the same as the $fpgd$ one, except that the neutron-$1d_{5/2}$ orbital is not active, and the

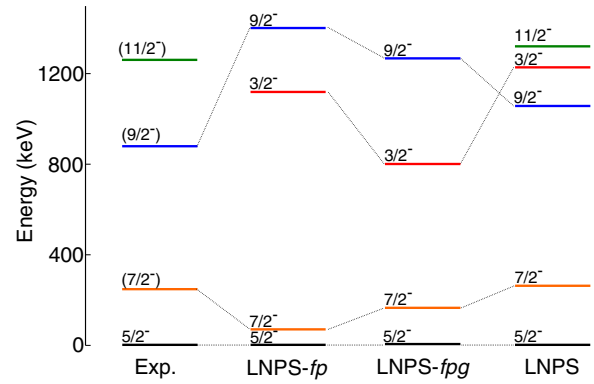

FIG. 7. Comparison of the proposed level scheme with shell-model calculations, see text for details. Spin-parity assignments for the upper two levels in the experimental scheme are tentative and based on the systematics of the lighter Mn isotopes and the shell-model calculations.

TABLE II. Experimental and shell-model transition energies, transition probabilities, multipole mixing ratios, branching ratios, and excited-state lifetimes using LNPS, LNPS-fpg, and LNPS-fp effective interactions for the $(7/2^-) \rightarrow 5/2^-$, $(9/2^-) \rightarrow (7/2^-)$, and $(11/2^-) \rightarrow (9/2^-)$ transitions discussed in the present work. Theoretical lifetimes $\tau_{\rm sm}$, branching ratios $BR_{\rm sm}$, and mixing ratios $\delta_{\rm sm}$ were calculated using both shell-model and experimental energies. The numbers without brackets were calculated using the shell-model energies, while the numbers in brackets are results of the same calculations but using the experimental level energies instead (see text for details). Experimentally determined lifetimes τ are listed for comparison.

Interaction	$J_i^\pi \rightarrow J_f^\pi$	$E_\gamma^{\rm expt}$ (MeV)	$E_\gamma^{\rm sm}$ (MeV)	$B(E2)_{\rm sm}$ (e^2 fm^4)	$B(M1)_{\rm sm}$ (μ_N^2)	$BR_{\rm sm}$ (%)	$\delta_{\rm sm}$	$\tau_{\rm sm}$ (ps)	τ (ps)
LNPS [13]	$(7/2^-) \rightarrow 5/2^-$	0.249(5)	0.262	467	0.13	100 [100]	0.13 [0.12]	23 [28]	8.5(0.5)
	$(9/2^-) \rightarrow (7/2^-)$	0.637(5)	0.795	323	0.29	92 [94]	0.22 [0.18]	0.3 [0.6]	0.9(0.6)
	$(11/2^-) \rightarrow (9/2^-)$	0.375(5)	0.262	274	0.48	26 [37]	0.05 [0.07]	1.7 [0.8]	<1
LNPS-fpg	$(7/2^-) \rightarrow 5/2^-$	0.249(5)	0.156	292	0.04	100 [100]	0.11 [0.17]	361 [88]	8.5(0.5)
	$(9/2^-) \rightarrow (7/2^-)$	0.637(5)	1.107	7	0.04	73 [80]	0.12 [0.07]	0.7 [4.4]	0.9(0.6)
LNPS-fp	$(7/2^-) \rightarrow 5/2^-$	0.249(5)	0.07	22	0.05	100 [100]	0.01 [0.04]	3165 [68]	8.5(0.5)
	$(9/2^-) \rightarrow (7/2^-)$	0.637(5)	1.33	10	0.02	91 [93]	0.27 [0.13]	1 [13]	0.9(0.6)

calculations are labeled "LNPS-fpg". Finally, calculations labeled "LNPS-fp" restrict the model space to the full fp shell for both protons and neutrons.

It has been demonstrated earlier that the fp model space is not sufficient to describe neutron-rich fp-shell nuclei in the vicinity of $N = 40$ (see, for example, Refs. [8,32–35]). In light of this observation, the LNPS-fp results reproduce the general low-energy structure of ^{63}Mn surprisingly well, while inclusion of the $0g_{9/2}$ orbital, as is done in calculations using the fpg model space, brings the $9/2^-$ level down in energy, closer to the experimental result. Only in the full LNPS calculations does the $11/2^-$ level appear in the calculations. Particularly curious is the behavior of the $3/2^-$ level in the calculations: when using only the fp model space (i.e., LNPS-fp), the state is calculated around 1 MeV, while the inclusion of the $0g_{9/2}$ neutron orbital lowers it down to 800 keV. In the full model space, with both the $0g_{9/2}$ and $1d_{5/2}$ neutron orbitals, the $3/2^-$ state is brought back well above 1 MeV. The calculated wave functions indicate that the $d_{5/2}$ amplitudes in the $5/2^-$, $7/2^-$, and $9/2^-$ states are significantly larger than those for the $3/2^-$ level. A $3/2^-$ state has not been identified in ^{63}Mn, so no experimental guidance can be given yet, but in ^{61}Mn, two levels with possible $3/2^-$ assignment are reported above 1 MeV [18].

To compare the data to the calculations in more depth, the excited-state lifetimes from the shell model are deduced and confronted with the measurement. The $(7/2^-) \rightarrow 5/2^-$ and $(9/2^-) \rightarrow (7/2^-)$ transitions are both expected to be of mixed $E2/M1$ multipolarity and from systematics (Fig. 6) are suspected to proceed with large branching ratios BR, defined as the intensity fraction to a specific final state. The $E2$-$M1$ multipole mixing ratio $\delta(E2/M1)$ is given by

$$\delta^2\left(\frac{E2}{M1}\right) = 6.87 \times 10^{-5}\, E_\gamma^2\, \frac{B(E2)}{B(M1)}\, \frac{\mu_N^2}{e^2\,\mathrm{fm}^4\,\mathrm{MeV}^2}, \quad (1)$$

and the lifetime of the state with the mixed $E2/M1$ transition is obtained as

$$\tau = BR\,\frac{\delta^2}{1+\delta^2}\,\frac{816}{E_\gamma^5\, B(E2; J+1 \rightarrow J)}\, e^2\,\mathrm{fm}^4\,\mathrm{MeV}^5\,\mathrm{ps}. \quad (2)$$

With the shell-model energies and transition probabilities in Eqs. (1) and (2), the mixing ratios and excited-state lifetimes were calculated and the lifetimes are compared to experiment (see Table II). The shell-model $B(E2)$ values used effective charges of $e_p = 1.31e$ and $e_n = 0.46e$ of Ref. [36], and the $B(M1)$ strengths were computed using effective g factors, $g_p^s = 4.189$, $g_n^s = -2.869$, $g_p^\ell = 1.1$, and $g_n^\ell = -0.1$.

The lifetimes calculated with the LNPS effective interaction give the best agreement with the experiment. For the $(7/2^-) \rightarrow 5/2^-$ transition, the LNPS lifetime of 23 ps over predicts the experimental value of 8.5(0.5) ps by a factor of 2.7, rather than by the factors of 42 and 372 found for the LNPS-fpg and LNPS-fp predictions, respectively. For the $(9/2^-) \rightarrow (7/2^-)$ transition, the LNPS prediction of 0.3 ps is also consistent with the measured value of 0.9(0.6) ps.

To remove the effect of the shell-model energies, the branching ratios, mixing ratios, and excited-state lifetimes are recalculated and given in brackets in Table II using the experimental excited-state energies instead of shell-model ones. With this modification, the overall agreement for the $(7/2^-) \rightarrow 5/2^-$ lifetime comes closer to the experiment for the interactions without the $1d_{5/2}$ orbital. For the $(9/2^-) \rightarrow (7/2^-)$ transition, however, only the LNPS prediction is consistent with the measured value.

In a simple single-particle picture, one may expect the low-lying structure of ^{63}Mn to be dominated by the three $f_{7/2}$ proton holes and their couplings. In this picture, the $5/2^-$ ground state then would have seniority 3 and the $(7/2^-)$ excited level would have seniority 1. In the extreme $(f_{7/2})^3$ limit, the $(7/2^-) \rightarrow 5/2^-$ transition is of forbidden $M1$ character; i.e., $B(M1) = 0$, since the seniority is pure and a transition would change it by two units. Although the LNPS-fpg and LNPS-fp calculations predict small $B(M1)$ values, the wave functions indicate already significant mixing in the proton configurations, beyond the $(f_{7/2})^3$ picture. The larger $B(M1)$ value for LNPS is a result of further mixing, favored by the excitation of neutrons into the $g_{9/2}$ and the $d_{5/2}$ orbitals, generating more collective and deformed states. This underlines the need for a large model space for the description of this mass region where rapid changes in shape occur.

IV. SUMMARY

In summary, a γ-ray spectroscopy experiment was performed on ^{63}Mn and new transitions were observed. The 637-keV transition was placed firmly in the level scheme as feeding the first excited state. From systematics, and in agreement with the shell model, the corresponding excited state was assigned $(9/2^-)$. The 375-keV transition was tentatively placed in the level scheme feeding the $(9/2^-)$ level and an $(11/2^-)$ spin-parity assignment is suggested from the systematics of the lighter Mn isotopes. GEANT4 simulations were used to determine the lifetimes of the $(7/2^-)$, $(9/2^-)$, and $(11/2^-)$ states from the γ-ray line shapes of the Doppler-corrected transitions observed in the two rings of the SeGA array. Large-scale shell-model calculations were performed in the $fpgd$, fpg, and fp model spaces, and the predicted level schemes and theoretical lifetimes for the excited states were compared to the data. While the excitation energies are dependent on the model space, the importance of the $\nu 0g_{9/2}$ and $\nu 1d_{5/2}$ orbitals was revealed more clearly in the comparison of the excited-state lifetimes. The calculations in the full $fpgd$ model space with the LNPS effective interaction give the best overall agreement with all experimental data, including the level lifetimes.

ACKNOWLEDGMENTS

This work was funded by the NSF under contracts PHY-0606007 and PHY-1102511, by the U.S. DOE, Office of Nuclear Physics, under contracts DE-AC02-06CH11357,DE-FG02-08ER41556, DE-FG02-94R40834, and by the U.K. Science and Technology Facilities Council (STFC).

[1] O. Sorlin and M.-G. Porquet, Prog. Part. Nucl. Phys. **61**, 602 (2008).
[2] A. Gade and T. Glasmacher, Prog. Part. Nucl. Phys. **60**, 161 (2008).
[3] T. Otsuka, T. Suzuki, R. Fujimoto, H. Grawe, and Y. Akaishi, Phys. Rev. Lett. **95**, 232502 (2005).
[4] N. Smirnova, B. Bally, K. Heyde, F. Nowacki, and K. Sieja, Phys. Lett. B **686**, 109 (2010).
[5] O. Sorlin, S. Leenhardt, C. Donzaud, J. Duprat, F. Azaiez, F. Nowacki, H. Grawe, Z. Dombrádi, F. Amorini, A. Astier, D. Baiborodin, M. Belleguic, C. Borcea, C. Bourgeois, D. M. Cullen, Z. Dlouhy, E. Dragulescu, M. Górska, S. Grévy, D. Guillemaud-Mueller, G. Hagemann, B. Herskind, J. Kiener, R. Lemmon, M. Lewitowicz, S. M. Lukyanov, P. Mayet, F. de Oliveira Santos, D. Pantalica, Y.-E. Penionzhkevich, F. Pougheon, A. Poves, N. Redon, M. G. Saint-Laurent, J. A. Scarpaci, G. Sletten, M. Stanoiu, O. Tarasov, and C. Theisen, Phys. Rev. Lett. **88**, 092501 (2002).
[6] O. Sorlin, C. Donzaud, F. Nowacki, J. Angélique, F. Azaiez, C. Bourgeois, V. Chiste, Z. Dlouhy, S. Grévy, D. Guillemaud-Mueller, F. Ibrahim, K.-L. Kratz, M. Lewitowicz, S. Lukyanov, J. Mrasek, Y.-E. Penionzhkevich, F. de Oliveira Santos, B. Pfeiffer, F. Pougheon, A. Poves, M. Saint-Laurent, and M. Stanoiu, Eur. Phys. J. A **16**, 55 (2003).
[7] P. Adrich, A. M. Amthor, D. Bazin, M. D. Bowen, B. A. Brown, C. M. Campbell, J. M. Cook, A. Gade, D. Galaviz, T. Glasmacher, S. McDaniel, D. Miller, A. Obertelli, Y. Shimbara, K. P. Siwek, J. A. Tostevin, and D. Weisshaar, Phys. Rev. C **77**, 054306 (2008).
[8] A. Gade, R. V. F. Janssens, T. Baugher, D. Bazin, B. A. Brown, M. P. Carpenter, C. J. Chiara, A. N. Deacon, S. J. Freeman, G. F. Grinyer, C. R. Hoffman, B. P. Kay, F. G. Kondev, T. Lauritsen, S. McDaniel, K. Meierbachtol, A. Ratkiewicz, S. R. Stroberg, K. A. Walsh, D. Weisshaar, R. Winkler, and S. Zhu, Phys. Rev. C **81**, 051304(R) (2010).
[9] W. Rother, A. Dewald, H. Iwasaki, S. M. Lenzi, K. Starosta, D. Bazin, T. Baugher, B. A. Brown, H. L. Crawford, C. Fransen, A. Gade, T. N. Ginter, T. Glasmacher, G. F. Grinyer, M. Hackstein, G. Ilie, J. Jolie, S. McDaniel, D. Miller, P. Petkov, T. Pissulla, A. Ratkiewicz, C. A. Ur, P. Voss, K. A. Walsh, D. Weisshaar, and K.-O. Zell, Phys. Rev. Lett. **106**, 022502 (2011).
[10] T. Baugher, A. Gade, R. V. F. Janssens, S. M. Lenzi, D. Bazin, B. A. Brown, M. P. Carpenter, A. N. Deacon, S. J. Freeman, T. Glasmacher, G. F. Grinyer, F. G. Kondev, S. McDaniel, A. Poves, A. Ratkiewicz, E. A. McCutchan, D. K. Sharp, I. Stefanescu, K. A. Walsh, D. Weisshaar, and S. Zhu, Phys. Rev. C **86**, 011305(R) (2012).
[11] H. L. Crawford, R. M. Clark, P. Fallon, A. O. Macchiavelli, T. Baugher, D. Bazin, C. W. Beausang, J. S. Berryman, D. L. Bleuel, C. M. Campbell, M. Cromaz, G. de Angelis, A. Gade, R. O. Hughes, I. Y. Lee, S. M. Lenzi, F. Nowacki, S. Paschalis, M. Petri, A. Poves, A. Ratkiewicz, T. J. Ross, E. Sahin, D. Weisshaar, K. Wimmer, and R. Winkler, Phys. Rev. Lett. **110**, 242701 (2013).
[12] B. Pritychenko, J. Choquette, M. Horoi, B. Karamy, and B. Singh, At. Data Nucl. Data Tables **98**, 798 (2012).
[13] S. M. Lenzi, F. Nowacki, A. Poves, and K. Sieja, Phys. Rev. C **82**, 054301 (2010).
[14] F. Recchia, S. M. Lenzi, S. Lunardi, E. Farnea, A. Gadea, N. Mărginean, D. R. Napoli, F. Nowacki, A. Poves, J. J. Valiente-Dobón, M. Axiotis, S. Aydin, D. Bazzacco, G. Benzoni, P. G. Bizzeti, A. M. Bizzeti-Sona, A. Bracco, D. Bucurescu, E. Caurier, L. Corradi, G. de Angelis, F. Della Vedova, E. Fioretto, A. Gottardo, M. Ionescu-Bujor, A. Iordachescu, S. Leoni, R. Mărginean, P. Mason, R. Menegazzo, D. Mengoni, B. Million, G. Montagnoli, R. Orlandi, G. Pollarolo, E. Sahin, F. Scarlassara, R. P. Singh, A. M. Stefanini, S. Szilner, C. A. Ur, and O. Wieland, Phys. Rev. C **85**, 064305 (2012).
[15] J. J. Valiente-Dobón, S. M. Lenzi, S. J. Freeman, S. Lunardi, J. F. Smith, A. Gottardo, F. D. Vedova, E. Farnea, A. Gadea, D. R. Napoli, M. Axiotis, S. Aydin, D. Bazzacco, P. G. Bizzeti, A. M. Bizzeti-Sona, G. Benzoni, D. Bucurescu, L. Corradi, A. N. Deacon, G. De Angelis, E. Fioretto, B. Guiot, M. Ionescu-Bujor, A. Iordachescu, S. Leoni, N. Mărginean, R. Mărginean, P. Mason, R. Menegazzo, D. Mengoni, B. Million, G. Montagnoli, R. Orlandi, F. Recchia, E. Sahin, F. Scarlassara, R. P. Singh, A. M. Stefanini, D. Steppenbeck, S. Szilner, C. A. Ur, B. J. Varley, and O. Wieland, Phys. Rev. C **78**, 024302 (2008).
[16] D. Steppenbeck, A. N. Deacon, S. J. Freeman, R. V. F. Janssens, S. Zhu, M. P. Carpenter, P. Chowdhury, M. Honma, T. Lauritsen, C. J. Lister, D. Seweryniak, J. F. Smith, S. L. Tabor, and B. J. Varley, Phys. Rev. C **81**, 014305 (2010).

[17] C. J. Chiara, I. Stefanescu, N. Hoteling, W. B. Walters, R. V. F. Janssens, R. Broda, M. P. Carpenter, B. Fornal, A. A. Hecht, W. Królas, T. Lauritsen, T. Pawłat, D. Seweryniak, X. Wang, A. Wöhr, J. Wrzesiński, and S. Zhu, Phys. Rev. C **82**, 054313 (2010).

[18] H. L. Crawford, P. F. Mantica, J. S. Berryman, R. Broda, B. Fornal, C. R. Hoffman, N. Hoteling, R. V. F. Janssens, S. M. Lenzi, J. Pereira, J. B. Stoker, S. L. Tabor, W. B. Walters, X. Wang, and S. Zhu, Phys. Rev. C **79**, 054320 (2009).

[19] L. Gaudefroy, O. Sorlin, C. Donzaud, J. Angélique, F. Azaiez, C. Bourgeois, V. Chiste, Z. Dlouhy, S. Grévy, D. Guillemaud-Mueller, F. Ibrahim, K.-L. Kratz, M. Lewitowicz, S. Lukyanov, I. Matea, J. Mrasek, F. Nowacki, F. de Oliveira Santos, Y.-E. Penionzhkevich, B. Pfeiffer, F. Pougheon, M. Saint-Laurent, and M. Stanoiu, Eur. Phys. J. A **23**, 41 (2005).

[20] M. Honma, T. Otsuka, B. A. Brown, and T. Mizusaki, Phys. Rev. C **65**, 061301(R) (2002).

[21] M. Honma, T. Otsuka, B. Brown, and T. Mizusaki, Eur. Phys. J. A **25**, 499 (2005).

[22] C. Babcock, H. Heylen, J. Billowes, M. Bissell, K. Blaum, P. Campbell, B. Cheal, R. G. Ruiz, C. Geppert, W. Gins, M. Kowalska, K. Kreim, S. Lenzi, I. Moore, R. Neugart, G. Neyens, W. Nörtershäuser, J. Papuga, and D. Yordanov, Phys. Lett. B **750**, 176 (2015).

[23] D. J. Morrissey, B. M. Sherrill, M. Steiner, A. Stolz, and I. Wiedenhoever, Nucl. Instrum. Methods Phys. Res., Sect. B **204**, 90 (2003).

[24] D. Bazin, J. A. Caggiano, B. M. Sherrill, J. Yurkon, and A. Zeller, Nucl. Instrum. Methods Phys. Res., Sect. B **204**, 629 (2003).

[25] J. Yurkon, D. Bazin, W. Benenson, D. J. Morrissey, B. M. Sherrill, D. Swan, and R. Swanson, Nucl. Instrum. Methods Phys. Res., Sect. A **422**, 291 (1999).

[26] W. F. Mueller, J. A. Church, T. Glasmacher, D. Gutknecht, G. Hackman, P. G. Hansen, Z. Hu, K. L. Miller, and P. Quirin, Nucl. Instrum. Methods Phys. Res., Sect. A **466**, 492 (2001).

[27] G. Audi, O. Bersillon, J. Blachot, and A. Wapstra, Nucl. Phys. **729**, 3 (2003), the 2003 NUBASE and Atomic Mass Evaluations.

[28] E. Runte, K. L. Gippert, W. D. Schmidt-Ott, P. Tidemand-Petersson, L. Ziegeler, R. Kirchner, O. Klepper, P. O. Larsson, E. Roeckl, D. Schardt, N. Kaffrell, P. Peuser, M. Bernas, P. Dessagne, M. Langevin, and K. Rykaczewski, Nucl. Phys. **441**, 237 (1985).

[29] I. Lee, Nucl. Instrum. Methods Phys. Res., Sect. A **422**, 195 (1999).

[30] A. Gade, R. V. F. Janssens, D. Weisshaar, B. A. Brown, E. Lunderberg, M. Albers, V. M. Bader, T. Baugher, D. Bazin, J. S. Berryman, C. M. Campbell, M. P. Carpenter, C. J. Chiara, H. L. Crawford, M. Cromaz, U. Garg, C. R. Hoffman, F. G. Kondev, C. Langer, T. Lauritsen, I. Y. Lee, S. M. Lenzi, J. T. Matta, F. Nowacki, F. Recchia, K. Sieja, S. R. Stroberg, J. A. Tostevin, S. J. Williams, K. Wimmer, and S. Zhu, Phys. Rev. Lett. **112**, 112503 (2014).

[31] S. Agostinelli, J. Allison, K. Amako, J. Apostolakis, H. Araujo, P. Arce, M. Asai, D. Axen, S. Banerjee, G. Barrand, F. Behner, L. Bellagamba, J. Boudreau, L. Broglia, A. Brunengo, H. Burkhardt, S. Chauvie, J. Chuma, R. Chytracek, G. Cooperman, G. Cosmo, P. Degtyarenko, A. Dell'Acqua, G. Depaola, D. Dietrich, R. Enami, A. Feliciello, C. Ferguson, H. Fesefeldt, G. Folger, F. Foppiano, A. Forti, S. Garelli, S. Giani, R. Giannitrapani, D. Gibin, J. G. Cadenas, I. González, G. G. Abril, G. Greeniaus, W. Greiner, V. Grichine, A. Grossheim, S. Guatelli, P. Gumplinger, R. Hamatsu, K. Hashimoto, H. Hasui, A. Heikkinen, A. Howard, V. Ivanchenko, A. Johnson, F. Jones, J. Kallenbach, N. Kanaya, M. Kawabata, Y. Kawabata, M. Kawaguti, S. Kelner, P. Kent, A. Kimura, T. Kodama, R. Kokoulin, M. Kossov, H. Kurashige, E. Lamanna, T. Lampén, V. Lara, V. Lefebure, F. Lei, M. Liendl, W. Lockman, F. Longo, S. Magni, M. Maire, E. Medernach, K. Minamimoto, P. M. de Freitas, Y. Morita, K. Murakami, M. Nagamatu, R. Nartallo, P. Nieminen, T. Nishimura, K. Ohtsubo, M. Okamura, S. O'Neale, Y. Oohata, K. Paech, J. Perl, A. Pfeiffer, M. Pia, F. Ranjard, A. Rybin, S. Sadilov, E. D. Salvo, G. Santin, T. Sasaki, N. Savvas, Y. Sawada, S. Scherer, S. Sei, V. Sirotenko, D. Smith, N. Starkov, H. Stoecker, J. Sulkimo, M. Takahata, S. Tanaka, E. Tcherniaev, E. S. Tehrani, M. Tropeano, P. Truscott, H. Uno, L. Urban, P. Urban, M. Verderi, A. Walkden, W. Wander, H. Weber, J. Wellisch, T. Wenaus, D. Williams, D. Wright, T. Yamada, H. Yoshida, and D. Zschiesche, Nucl. Instrum. Methods Phys. Res., Sect. A **506**, 250 (2003).

[32] E. Caurier, F. Nowacki, and A. Poves, Eur. Phys. J. A **15**, 145 (2002).

[33] J. Ljungvall, A. Görgen, A. Obertelli, W. Korten, E. Clément, G. de France, A. Bürger, J.-P. Delaroche, A. Dewald, A. Gadea, L. Gaudefroy, M. Girod, M. Hackstein, J. Libert, D. Mengoni, F. Nowacki, T. Pissulla, A. Poves, F. Recchia, M. Rejmund, W. Rother, E. Sahin, C. Schmitt, A. Shrivastava, K. Sieja, J. J. Valiente-Dobón, K. O. Zell, and M. Zielińska, Phys. Rev. C **81**, 061301 (2010).

[34] S. Zhu, A. N. Deacon, S. J. Freeman, R. V. F. Janssens, B. Fornal, M. Honma, F. R. Xu, R. Broda, I. R. Calderin, M. P. Carpenter, P. Chowdhury, F. G. Kondev, W. Królas, T. Lauritsen, S. N. Liddick, C. J. Lister, P. F. Mantica, T. Pawłat, D. Seweryniak, J. F. Smith, S. L. Tabor, B. E. Tomlin, B. J. Varley, and J. Wrzesiński, Phys. Rev. C **74**, 064315 (2006).

[35] S. J. Freeman, R. V. F. Janssens, B. A. Brown, M. P. Carpenter, S. M. Fischer, N. J. Hammond, M. Honma, T. Lauritsen, C. J. Lister, T. L. Khoo, G. Mukherjee, D. Seweryniak, J. F. Smith, B. J. Varley, M. Whitehead, and S. Zhu, Phys. Rev. C **69**, 064301 (2004).

[36] M. Dufour and A. P. Zuker, Phys. Rev. C **54**, 1641 (1996).